CHARACTERIZING THE SPECTRAL RADIANCE OF LUNAR PERMANENTLY SHADOWED REGIONS P. Mahanti[1], H.M.Brown[1], M.S.Robinson[1], A.K. Boyd[1], D.Humm[2], A. Awumah[1], [1]LROC Science Operation Center, School of Earth and Space Exploration, Arizona State University, Tempe, Arizona (pmahanti.lroc@gmail.com);[2]Space Instrument Calibration Consulting, Annapolis, Maryland.

Introduction: The low obliquity of the Moon (1.54°) results in permanently shadowed regions (PSRs) in topographic lows at high latitudes [1, 2] (Figure 1). PSRs typically exist in the lower reaches of host craters while the upper reaches receive periods of solar illumination. Some permanent shadows have extremely low temperatures (measured mid-day brightness temperatures of 29 °K) and thus volatile molecules deposited from various sources (e.g. comet or asteroid impacts) can remain cold trapped [3]. Mapping the location, abundance, and species of volatiles within PSRs is a key goal of previous, ongoing, and upcoming lunar missions.

PSR temperatures (and cold-trap behavior) is controlled by scattered solar illumination bouncing off crater walls and other surrounding topography, emitted thermal energy from surrounding topography, and energy from the interior of the Moon [4]. By using topography based simulation of scattered light, the incoming flux at some PSRs (>200 m diameter) (irradiance; Wm^{-2} units) was characterized earlier [5] but a detailed observation based analysis characterizing the magnitudes of scattered solar illumination is absent. In this work we study the broadband visible (400−760 nm) spectral radiance (R; $Wm^{-2}sr^{-1}\mu m^{-1}$ units) within PSRs from scattered solar illumination.

PSR Imaging: The Lunar Reconnaissance Orbiter Camera (LROC) Narrow Angle Camera (NAC) obtains useful images of PSRs with long exposure observations during times of maximum secondary illumination [6]. The increased exposure time 1.01 ms to 35.3 ms) leads to elongated pixels in the along-track direction, thus pixel scale is increased compared to typical NAC images (10–40 m/pixel vs. 0.5 m/pixel). Typically, the 12-bit (0-4095) NAC values have sufficient dynamic range to capture and reveal landforms in both illuminated and shadowed terrains. A raw NAC image is converted to a radiance calibrated NAC image by using the USGS ISIS LRONACCAL module[7, 8]

The acquisition of NAC PSR observations has been refined over several campaigns to optimize the trade-off between signal-to-noise ratio (SNR) and pixel scale, resulting in a comprehensive dataset [9]. A total of 6,199 individual NAC PSR observations have been collected since the start of the mission through 1 October 2017. The NAC PSR images reviewed in this study include a total of 4,368 unique NAC observations that overlap PSRs >10 km^2, ranging from 81°N,S to 90°N,S. PSR

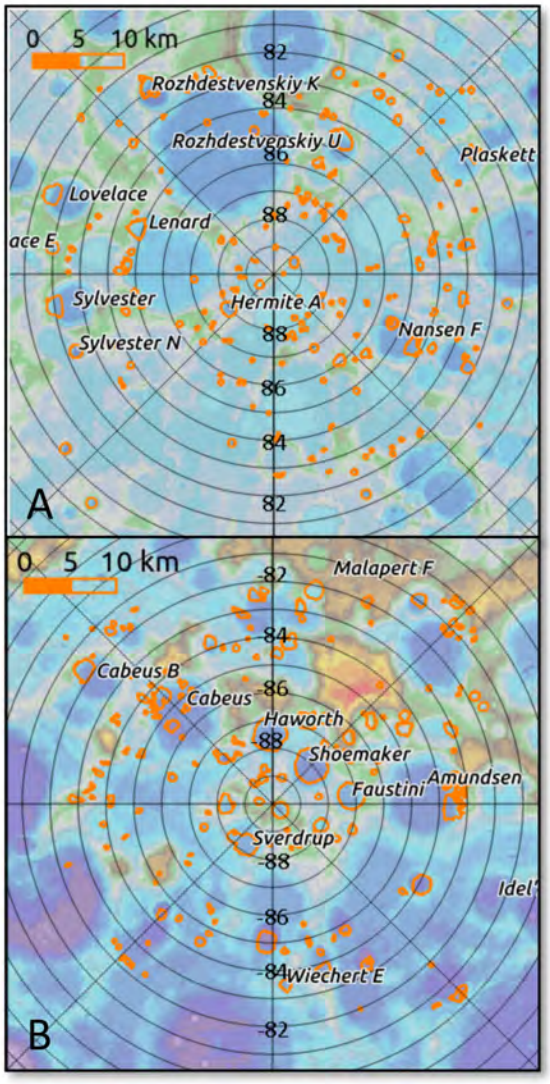

Figure 1: Polar stereographic views of the color shaded relief from the GLD 100, with LOLA PSR boundaries used in this study for the north pole (A) and south pole (B).

boundaries are identified from LOLA PSR shapefile [5] which is used to crop NAC images to PSRs.

Computing spectral statistics: A total of 5,940 cropped PSR regions (multiple NAC images and multiple PSRs) were used to derive the radiance statistics within the PSR masks. For each PSR and overlapping image combination, the median (50% signal value from CDF), lower-limit (LL; 2% signal value) and upper-limit (UL; 98% signal value) statistics were obtained (Figure 2). These radiance statistics were used to compute the radiance cumulative distribution func-

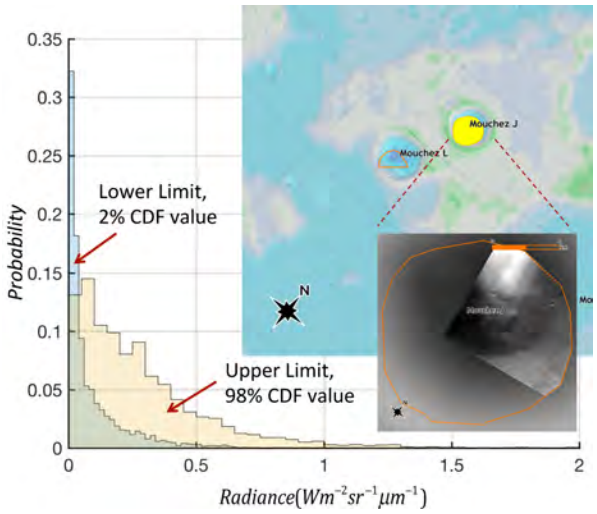

Figure 2: Distribution of Radiance UL (98%) and LL (2%) statistics. Inset shows an example of PSR outline (orange) partly imaged by a cropped NAC image.

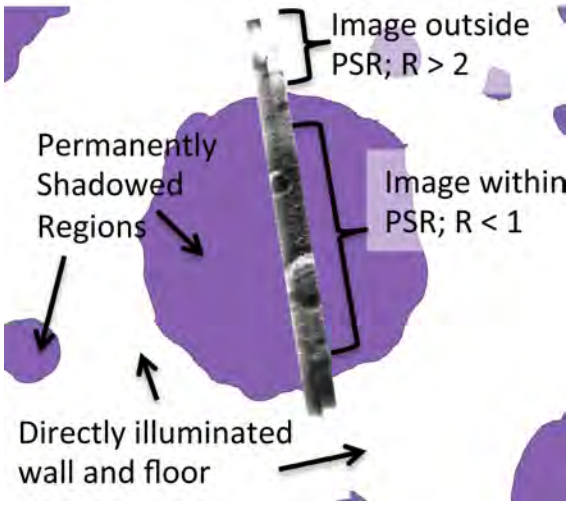

Figure 3: Radiance values on and outside the PSR within Shackleton crater.

tions (CDF). The value of the radiance signal depends on many factors. The most important ones are: (1) Solar position (latitude and longitude), (2) the angle of the orbital plane of LRO and the solar vector (β), (3) PSR latitude and longitude, and (4) Exposure time.

Results and Discussions: The median values of the 2% and 98% PSR scene radiance statistics are 0.04 and 0.2 $Wm^{-2}sr^{-1}\mu m^{-1}$ respectively, indicating the large number of pixels in most PSR images have $R < 0.2$. The maximum UL and LL values were 2.7 and 1.1 $Wm^{-2}sr^{-1}\mu m^{-1}$. The median radiance value from the NAC was 0.1 $Wm^{-2}sr^{-1}\mu m^{-1}$. Approximately 85% of the images have a dynamic range [2%, 98%] limits of 0.01 and 2 $Wm^{-2}sr^{-1}\mu m^{-1}$ and $Rvalues >$ 2 occur outside the PSRs (Figure 3). North pole PSRs

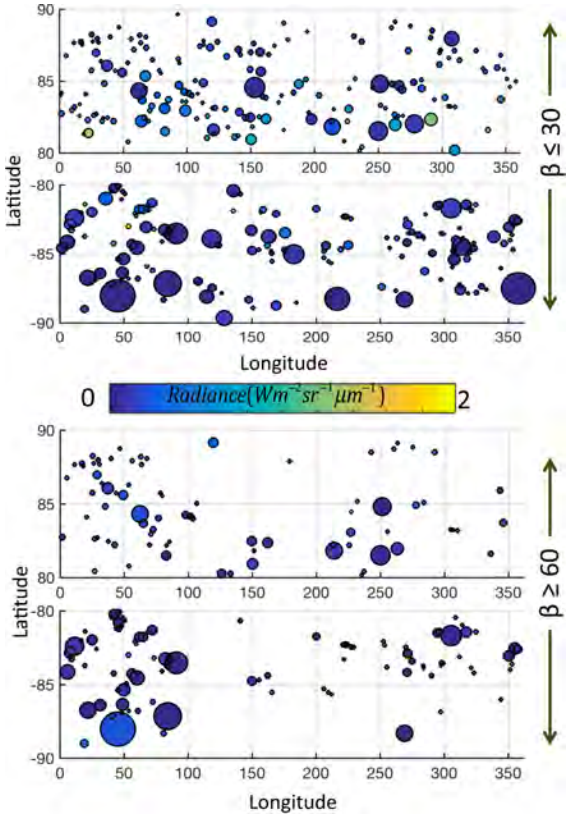

Figure 4: Radiance (UL statistics) at PSRs when images were acquired at high and low beta.

are typically smaller than south pole PSRs (median values of $25km^2$ and $77km^2$ for PSRs larger than $10km^2$) and are brighter as a group than south pole PSRs (Figure 4). When images are acquired at more acute β angles the disparity increases (UL values of 0.36 vs 0.15).

Conclusion: Imaging PSR scenes is challenging due to the minimal illumination at the PSRs (close to or below the detector limit) proximal to bright targets (illuminated terrain). The sensitivity and large dynamic range of the NAC helps PSR imaging, although at lower SNR and resolution compared to nominal NAC images. PSR scene radiance statistics computed in this work takes us a step further in being able to distinguish increased radiance levels from future PSR images of higher resolution and signal-to-noise ratio.

References: [1] H. UREY (1951) *Press Nueva Harven.* [2] K. Watson, et al. (1961) *Journal of Geophysical Research* 66(9):3033. [3] D. A. Paige, et al. (2010) *science* 330(6003):479. [4] A. R. Vasavada, et al. (1999) *Icarus* 141(2):179. [5] E. Mazarico, et al. (2011) *Icarus* 211(2):1066. [6] S. Koeber, et al. (2013) in *Lunar and Planetary Science Conference* vol. 44 2588. [7] L. Keszthelyi, et al. (2013) in *Lunar and Planetary Science Conference* vol. 44 2546. [8] J. Anderson, et al. (2004) in *Lunar and Planetary Science Conference* vol. 35. [9] S. Koeber, et al. (2014) in *Lunar and Planetary Science Conference* vol. 45 2811.